Kryžanowski, A., Saje, M., Planinc, I., Zupan, D. 2008. Analytical solution for buckling of asymmetrically delaminated Reissner's elastic columns including transverse shear. *International journal of solids and structures* 45,3-4: 1051-1070. DOI: 10.1016/j.ijsolstr.2007.09.027.

Analytical solution for buckling of asymmetrically delaminated Reissner's elastic columns including transverse shear

A. Kryžanowski, M. Saje, I. Planinc and D. Zupan*

University of Ljubljana, Faculty of Civil and Geodetic Engineering, Jamova 2, SI-1115 Ljubljana, Slovenia

Abstract

The exact analytical solution of buckling in delaminated columns is presented. In order to investigate analytically the influence of axial and shear strains on buckling loads the geometrically exact beam theory is employed with no simplification of the governing equations. The critical forces are then obtained by the linearized stability theory. In the paper we limit the studies to linear elastic columns with a single delamination, but with arbitrary longitudinal and vertical asymmetry of delamination and arbitrary boundary conditions. The studies of quantitative and qualitative influence of transverse shear are shown in detail and extensive results for buckling loads with respect to delamination length, thickness and longitudinal position are presented.

Key words: delamination, buckling, layered beam, shear deformation,

1 Introduction

Since Euler's work in buckling of elastic columns [8] the buckling and post-buckling analysis of structures has been a subject of research of many authors. Euler's results differ from the experimental ones due to material non-linearity, imperfections in geometry and loading eccentricities [1]. Better understanding of mechanical grounds for the failure of structures is especially important for design of modern structures, often build from modern-type composite materials. The use of laminated composites for instance or more generally a load carrying members with geometric imperfections can result in premature collapse

* Corresponding author. E-mail addresss: dejan.zupan@fgg.uni-lj.si

due to local instabilities. That is why the mathematical modelling of buckling and post-buckling considering different effects of non-linearity and imperfections has received considerable attention in the last decade, see, e.g. the publications by Chen [3] [4], Kardomateas and Schumueser [10], Lim and Parsons [14], Moradi and Taheri [15], Numayr and Haddad [16], MSRao et al. [17], MSRao and Shu [18], Sheinman and Soffer [21], Wang et al. [26].

The work by Chai and coworkers [2] represents a first attempt in modelling the delaminated beam. In [2] the energy release rate criterion is applied and the effect of delamination growth is also studied. The beam is divided into four regions and the continuity conditions at the delamination ends are applied. Similar delaminated beam model was used by Simitses et al. [22], where the effect of delamination length and vertical position is studied in detail for simply supported beams and the beams with clamped ends.

Kardomateas and Schumueser [10] and later Chen [3] have incorporated the transverse shear effect into their studies. Kardomateas and Schumueser [10] studies are based on classical Euler's solution, Chen [3] used the a variational energy principle instead. Both papers employ the Griffith-type fracture criterion for studying the delamination growth. Later Chen [4] used the first order shear deformation theory to develop closed-form expressions for buckling and post-buckling of asymmetrically delaminated beams with clamped boundary. Moradi and Taheri [15] solved the same problem by the differential quadrature method.

The objective of the present paper is twofold: to derive the exact analytical solution for the buckling of single-delaminated column with consistent consideration of transverse shear, and to investigate the effect of delamination length position and shear effect on buckling loads. In contrast to other authors we here employ the linearized stability theory [11] and present the exact analytical solution with no simplification of the governing equations. We restrict our analysis to the buckling analysis of linear elastic columns with a single asymmetric delamination and arbitrary boundary conditions. The post-buckling analysis is not the issue of the present paper. The extension of the present formulation on multiple delamination and composites made of several materials with different material properties can easily be made.

2 Problem definition

We consider straight column with constant cross-section and compressive axial force F, acting along the neutral axis of the column (Figure 1). The column is divided by a single delamination into four elements. Elements 1 and 4 represent both non-delaminated ends of the column. Elements 2 and 3 represent the

two layers at the middle of the column. Delamination is parallel to the neutral axis of the column, but otherwise placed at an arbitrary position. Relative delamination length is defined by $d.l. = \frac{L_2}{L}$, where L denotes the total length of the column. The asymmetry of delamination with respect to the height of the column is uniquely described by parameter $\mu \in (-1, 1)$. $\mu = 0$ means the vertically symmetrical delamination, by increasing (or decreasing) the value of μ, the delamination is moved along the height of the column towards the boundary. The longitudinal asymmetry is defined by the ratio of the undelaminated ends $a = L_1/L_4$. $a = 1$ means longitudinally symmetrical delamination, delamination is positioned nearer left end for $a \in (0, 1)$ and nearer right end for $a > 1$.

Global coordinate system (X, Y, Z) is chosen, in which the undeformed centroidal axis lies in the plane XZ, X-axis is perpendicular to the neutral axis of the column, Y-axis points out of the figure, and the reference point $(0, 0, 0)$ coincides with the bottom of the column. Local coordinate system (x, y, z) is assumed to coincide initially with global coordinates, and then follows the deformation of the beam. Plane cross-sections are assumed to remain planar and preserve their shape and area after the deformation. The column is made of

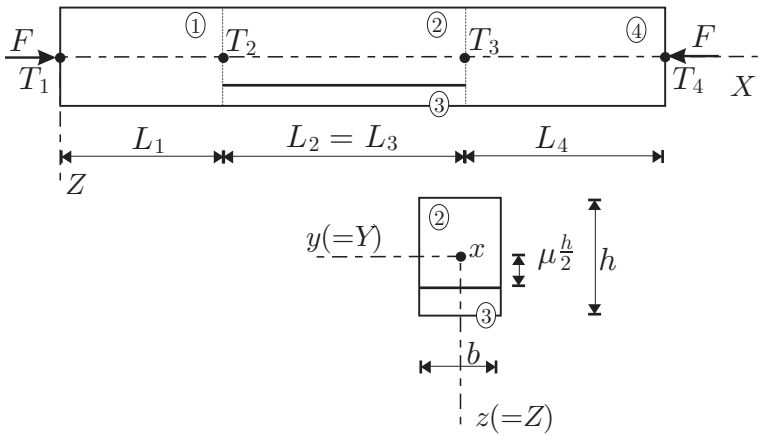

Fig. 1. Model of the column with single asymmetric delamination.

linearly elastic homogenous material. The smallest point load, called the critical force, is sought, such that the buckling of the column occurs. Note that both layers are initially straight and that contact along the length of layers can occur only at the post-buckling stage. Note that the present model assumes that the delaminated layers deforms freely and have different transverse deformations. This assumption may not be practical due to the overlapping of the delaminated layers [25] in the post-buckling analysis which is, however, not the issue of the present paper.

3 Analytical solution

3.1 Governing equations

The present solution is based on the stability analysis of the exact analytical solution of the linearized planar beam theory. We stem from non-linear planar Reissner beam theory and describe the beam by:

i) *kinematic equations*

$$1 + u' = (1 + \varepsilon)\cos\varphi + \gamma \sin\varphi \tag{1}$$
$$w' = -(1 + \varepsilon)\sin\varphi + \gamma\cos\varphi \tag{2}$$
$$\varphi' = \kappa, \tag{3}$$

ii) *equilibrium equations*

$$R'_X + p_X = 0 \tag{4}$$
$$R'_Z + p_Z = 0 \tag{5}$$
$$M' - (1 + \varepsilon)Q + \gamma N - m_Y = 0, \tag{6}$$

where

$$N = R_X \cos\varphi - R_Z \sin\varphi \tag{7}$$
$$Q = R_X \sin\varphi + R_Z \cos\varphi, \tag{8}$$

iii) and *constitutive equations*

$$N = E \int_A (\varepsilon + z\kappa)\, dA \tag{9}$$
$$Q = GA_s\gamma \tag{10}$$
$$M = E \int_A z\,(\varepsilon + z\kappa)\, dA. \tag{11}$$

Here

- E and G denote elastic and shear moduli of material;
- A is the cross-sectional area;
- A_s is the effective shear area [7];
- u and w denote the displacements of the beam;
- φ is the rotation;
- ε is the extensional strain, γ is the shear strain, κ is the bending strain (curvature);
- p_X, p_Z and m_Y are external distributed forces and moments, respectively;
- R_X, R_Z and M are the stress-resultant forces and moment.

Note that, when expressed with respect to the local basis, the stress forces are denoted by N and Q and related to R_X and R_Z by coordinate transformation (7)–(8).

After considering that the column is loaded only by point loads and employing some simple eliminations we obtain the complete set of non-linear governing equations

$$1 + u' - (1+\varepsilon)\cos\varphi - \gamma\sin\varphi = 0 \tag{12}$$
$$w' + (1+\varepsilon)\sin\varphi - \gamma\cos\varphi = 0 \tag{13}$$
$$\varphi' - \kappa = 0 \tag{14}$$
$$R_X' = 0 \tag{15}$$
$$R_Z' = 0 \tag{16}$$
$$M' + w'R_X - (1+u')R_Z = 0 \tag{17}$$
$$E\int_A (\varepsilon + z\kappa)\, dA - R_X\cos\varphi + R_Z\sin\varphi = 0 \tag{18}$$
$$GA_s\gamma - R_X\sin\varphi - R_Z\cos\varphi = 0 \tag{19}$$
$$E\int_A z\,(\varepsilon + z\kappa)\, dA - M = 0. \tag{20}$$

The critical points of the non-linear set of equations agree with the critical points of the linearized system [11]. For the application of linearized stability theory in existence and uniqueness of the solution of Reissner's elastica see the paper by Flajs et al. [9].

3.2 Linearized equations

Similarly as in paper by Zupan and Saje [28] for three-dimensional beams, consistent variation of equations (12)–(19) will be employed at an arbitrary configuration of the beam. The deduction of the variations is simplified if variations of constitutive equations are prepared in advance:

$$\delta N = C_{11}\delta\varepsilon + C_{12}\delta\kappa \tag{21}$$
$$\delta M = C_{21}\delta\varepsilon + C_{22}\delta\kappa, \tag{22}$$

where

$$C_{11} = \frac{\partial N}{\partial\varepsilon} = E\int_A \frac{\partial}{\partial\varepsilon}(\varepsilon + z\kappa)\, dA = EA \tag{23}$$
$$C_{12} = \frac{\partial N}{\partial\kappa} = E\int_A \frac{\partial}{\partial\kappa}(\varepsilon + z\kappa)\, dA = E\int_A z\, dA = ES_y \tag{24}$$
$$C_{21} = \frac{\partial N}{\partial\varepsilon} = E\int_A \frac{\partial}{\partial\varepsilon}\left(z\varepsilon + z^2\kappa\right) dA = E\int_A z\, dA = ES_y \tag{25}$$

$$C_{22} = \frac{\partial M}{\partial \kappa} = E \int_A \frac{\partial}{\partial \kappa} \left(z\varepsilon + z^2 \kappa \right) \, dA = E \int_A z^2 \, dA = E I_y. \tag{26}$$

Here S_y denotes the moment of area and I_y the moment on inertia. Note that S_y is not zero for all the layers where the centroidal axis does not coincide with the neutral axis of the whole beam. C_{11}, C_{12}, C_{21}, and C_{22} are the components of the cross-section constitutive tangent matrix. It's determinant

$$c = C_{11} C_{22} - C_{12} C_{21} \tag{27}$$

is crucial for observing the failure at the cross-section. Here, it is suitable to introduce the notation

$$d = \frac{c}{C_{11}} \tag{28}$$

for the constitutive tangent matrix determinant divided by the axial stiffness. Note also that the axial stiffness is strictly positive quantity. As reported by Krauberger et al., the non-linearity of material could considerably affect buckling and post-buckling behaviour of frame structures. The present approach could easily be extended to non-linear material due to consistent linearization of constitutive equations introduced above.

After these preparations the variations of the equations of the beam are easily derived and are as follows:

$$\delta u' - w' \delta \varphi - \cos\varphi \, \delta\varepsilon - \sin\varphi \, \delta\gamma = 0 \tag{29}$$

$$\delta w' + (1 + u') \, \delta\varphi + \sin\varphi \, \delta\varepsilon - \cos\varphi \, \delta\gamma = 0 \tag{30}$$

$$\delta\varphi' - \delta\kappa = 0 \tag{31}$$

$$\delta R_X' = 0 \tag{32}$$

$$\delta R_Z' = 0 \tag{33}$$

$$\delta M' + R_X \delta w' - R_Z \delta u' + w' \delta R_X - (1 + u') \delta R_Z = 0 \tag{34}$$

$$C_{11}\delta\varepsilon + C_{12}\delta\kappa + (R_X \sin\varphi + R_Z \cos\varphi) \, \delta\varphi - \cos\varphi \, \delta R_X + \sin\varphi \, \delta R_Z = 0 \tag{35}$$

$$GA_s \delta\gamma - (R_X \cos\varphi - R_Z \sin\varphi) \, \delta\varphi - \sin\varphi \, \delta R_X - \cos\varphi \, \delta R_Z = 0 \tag{36}$$

$$C_{21}\delta\varepsilon + C_{22}\delta\kappa - \delta M = 0. \tag{37}$$

The linearized equations (29)–(37) can be evaluated at an arbitrary configuration of the beam. In order to apply equations to the column buckling problem, the linearized equations are to be evaluated at the primary configuration of the column. The primary configuration of the column is an arbitrary deformed configuration in which the column is straight

$$\varphi(x) = 0, \quad w(x) = 0 \tag{38}$$

an loaded only along the neutral axis

$$R_Z(x) = 0, \quad M(x) = 0. \tag{39}$$

By inserting (38) and (39) into equations (12)–(19) we have

$$\kappa(x) = 0 \tag{40}$$
$$\gamma(x) = 0 \tag{41}$$
$$u'(x) = \varepsilon(x) = const \tag{42}$$
$$R_X(x) = const \tag{43}$$

Combining (38)–(43) and (29)–(37) gives linearized equations at primary configuration:

$$\delta u' - \delta\varepsilon = 0 \tag{44}$$
$$\delta w' + (1+\varepsilon)\,\delta\varphi - \delta\gamma = 0 \tag{45}$$
$$\delta\varphi' - \delta\kappa = 0 \tag{46}$$
$$\delta R_X' = 0 \tag{47}$$
$$\delta R_Z' = 0 \tag{48}$$
$$\delta M' + R_X\delta w' - (1+\varepsilon)\delta R_Z = 0 \tag{49}$$
$$C_{11}\delta\varepsilon + C_{12}\delta\kappa - \delta R_X = 0 \tag{50}$$
$$GA_s\delta\gamma - R_X\delta\varphi - \delta R_Z = 0 \tag{51}$$
$$C_{21}\delta\varepsilon + C_{22}\delta\kappa - \delta M = 0. \tag{52}$$

Equations (44)–(49) represent system of six ordinary differential equations for nine unknown functions of x: δu, δw, $\delta\varphi$, δR_X, δR_Z, δM. Algebraic equations (50)–(52) are linearized constitutive equations that represents relations between δR_X, δR_Z, δM and $\delta\varepsilon$, $\delta\gamma$, $\delta\kappa$. Due to the simple form of (44)–(52) they can be solved analytically.

3.3 Analytical solution of linearized equations

The set of nine equations (44)–(52) will be transformed into only two differential equations of higher order. The only remaining unknown will be axial and lateral deflections δu and δw. By taking the first derivative of equation (45), the first derivative of (51), and (48) we have

$$\delta w'' = \left[-(1+\varepsilon) + \frac{R_X}{GA_s}\right]\delta\varphi' = \left[-(1+\varepsilon) + \frac{R_X}{GA_s}\right]\delta\kappa \tag{53}$$

and

$$\delta w^{(iv)} = \left[-(1+\varepsilon) + \frac{R_X}{GA_s}\right]\delta\kappa''. \tag{54}$$

Second derivative of (52) gives

$$\delta M'' = C_{21}\delta\varepsilon'' + C_{22}\delta\kappa'', \tag{55}$$

on the other hand from (49) and (48) it follows that

$$\delta M'' = -R_X \delta w''. \tag{56}$$

The equality of right hand sides in (55) and (56) gives

$$C_{21}\delta\varepsilon'' + C_{22}\delta\kappa'' + R_X\delta w'' = 0. \tag{57}$$

Finally by inserting (50) and (54) into (57) and considering (28), we get

$$d\,\delta w^{(iv)} + R_X\left[-(1+\varepsilon) + \frac{R_X}{GA_s}\right]\delta w'' = 0. \tag{58}$$

If we introduce the buckling parameter

$$\boxed{k^2 = -\frac{R_X}{d}\left[(1+\varepsilon) - \frac{R_X}{GA_s}\right],} \tag{59}$$

fourth order differential equation (58) can be written in a simple form as:

$$\delta w^{(iv)} + k^2\delta w'' = 0. \tag{60}$$

Equation (60) can be solved analytically; the solution is

$$\boxed{\delta w\,(x) = A\sin kx + B\cos kx + Cx + D.} \tag{61}$$

Four parameters A, B, C, and D must be determined form the boundary conditions. Various boundary conditions, presented in the next section, need to be analyzed: different supports at both ends of the column and the bonding conditions between middle layers and the elements at both ends. It is obvious from the general approach that the solution (61) holds for all four elements composing the column. However due to different boundary conditions each element has different parameters. Thus, sixteen parameters A_i, B_i, C_i, and D_i, $i = 1, \ldots, 4$ uniquely define the lateral deflection of the column.

Taking the first derivative of (50) and considering (44) and (47) gives

$$C_{11}\delta u'' + C_{12}\delta\kappa' = 0.$$

From (53) we then obtain

$$\frac{C_{11}}{C_{12}}\left[-(1+\varepsilon) + \frac{R_X}{GA_s}\right]\delta u'' + \delta w''' = 0.$$

After inserting the solution for δw (61) and taking into account (59) we finally get

$$\delta u'' = \frac{R_X C_{12}}{d\, C_{11}} k \left(A \cos kx - B \sin kx \right). \tag{62}$$

Exact solution of the second order equation (62) reads

$$\boxed{\delta u\left(x\right) = \alpha + \beta x - \frac{R_X C_{12}}{k\, d\, C_{11}} \left(A \cos kx - B \sin kx \right),} \tag{63}$$

where the two parameters α and β are to be determined from the boundary equations. Again each element could have different values of parameters α and β. All together eight parameters α_i, β_i, $i = 1, \ldots, 4$ uniquely define the axial deflection of the column.

An arbitrary deformed configuration of the linearized beam is uniquely described by $\delta w\left(x\right)$, $\delta u\left(x\right)$, and the boundary conditions. The remaining quantities of the beam $\delta\varphi$, δR_X, δR_Z, δM can be obtained from (44)–(52). It is, however, suitable to directly express those quantities with δu, δw, and their derivatives as we will employ these expressions in order to properly consider the physical boundary and bonding conditions.

Firstly, we express δR_Z from (49)

$$\delta R_Z = \frac{R_X}{1+\varepsilon} \delta w' + \frac{1}{1+\varepsilon} \delta M'. \tag{64}$$

$\delta M'$ can further be expressed from (52) and considering (50) and (47) as

$$\delta M' = d\, \delta \kappa'. \tag{65}$$

From (53), (64), and (65) now follows

$$\begin{aligned} \delta R_Z &= \frac{R_X}{1+\varepsilon} \delta w' + \frac{d}{\left(1+\varepsilon\right) \left[-\left(1+\varepsilon\right) + \frac{R_X}{G A_s} \right]} \delta w''' \\ \delta R_Z &= \frac{R_X}{1+\varepsilon} \left(\delta w' + \frac{1}{k^2} \delta w''' \right). \end{aligned} \tag{66}$$

Inserting the solution for δw into (66) results in

$$\boxed{\delta R_Z = \frac{R_X}{1+\varepsilon} C.} \tag{67}$$

From (44) we have

$$\delta\gamma = \delta w' + \left(1+\varepsilon\right) \delta\varphi \tag{68}$$

and on the other hand from (51) we get

$$\delta\gamma = \frac{R_X}{GA_s}\delta\varphi + \frac{1}{GA_s}\,\delta R_Z. \tag{69}$$

Upon insertion (69) and (66) into (68) and some short simplification where (59) is taken into account, it yields

$$\delta\varphi = -\frac{1}{1+\varepsilon}\left[\delta w' + \frac{R_X^2}{GA_s k^4 d}\delta w'''\right]. \tag{70}$$

After we insert the solution (61) into (70) and rearrange the terms, we obtain

$$\boxed{\delta\varphi = \frac{R_X}{k\,d}\left(A\cos kx - B\sin kx\right) - \frac{1}{1+\varepsilon}C.} \tag{71}$$

By inserting (44) and (53) into (52) we have

$$\delta M = C_{21}\delta u' + C_{22}\frac{R_X}{k^2 d}\delta w'' \tag{72}$$

and in completely analogous way

$$\delta R_X = C_{11}\delta u' + C_{12}\frac{R_X}{k^2 d}\delta w''. \tag{73}$$

It is suitable to insert solutions (61)–(63) into (72) and (73) as the expression simplify considerably. After some short derivations we directly obtain

$$\boxed{\delta R_X = C_{11}\beta} \tag{74}$$

$$\boxed{\delta M = C_{21}\beta - R_X\left(A\sin kx + B\cos kx\right).} \tag{75}$$

4 Boundary and continuity conditions

Before we discuss the conditions on linearized formulation the continuity of displacements and equilibrium of forces in non-linear primary configuration need to be considered. Continuity of displacements at the delamination ends (points T_2 and T_3 on Figure 1) reads:

$$\begin{aligned} u_1\left(L_1\right) &= u_2\left(0\right) = u_3\left(0\right) \\ u_2\left(L_2\right) &= u_3\left(L_2\right) = u_4\left(0\right). \end{aligned}$$

From (12) and (38) we have

$$\begin{aligned} u' &= \varepsilon \\ u(x) &= u(0) + \varepsilon x. \end{aligned} \tag{76}$$

As one end of column is fixed, we have

$$u_1(0) = 0,$$

and inserting (76) into continuity conditions yields

$$\begin{aligned} \varepsilon_1 L_1 &= u_2(0) = u_3(0) \\ u_2(0) + \varepsilon_2 L_2 &= u_3(0) + \varepsilon_3 L_2 = u_4(0). \end{aligned}$$

Thus the axial strains of both layers are equal

$$\varepsilon_2 = \varepsilon_3. \tag{77}$$

Equilibrium conditions of axial forces at points T_2, T_3, and T_4 are

$$R_{X,2} + R_{X,3} = R_{X,1} \tag{78}$$
$$R_{X,2} + R_{X,3} = R_{X,4} \tag{79}$$
$$R_{X,4} = -F. \tag{80}$$

The axial forces can be expressed with axial strains. From (38)–(43) and (18) we obtain

$$R_{X,i} = EA_i\varepsilon_i, \quad \text{for } i = 1, \ldots, 4. \tag{81}$$

By inserting (81) into (78)–(79) and considering (77) we get

$$\begin{aligned} EA_2\varepsilon_2 + EA_3\varepsilon_2 &= EA_1\varepsilon_1 \\ EA_2\varepsilon_2 + EA_3\varepsilon_2 &= EA_4\varepsilon_4. \end{aligned}$$

As for columns with constant cross-sections $A_2 + A_3 = A_1 = A_4$, we finally have the continuity of axial strains

$$\varepsilon_1 = \varepsilon_2 = \varepsilon_3 = \varepsilon_4. \tag{82}$$

From (81) and (82) now follows

$$R_{X,1} = -F \tag{83}$$
$$R_{X,2} = -\frac{A_2}{A_4}F \tag{84}$$
$$R_{X,3} = -\frac{A_3}{A_4}F. \tag{85}$$

As reported by Li [13] the exact solution for buckling considering the effect of shear can not be easily obtained for non-uniform bar, especially for multi-step bars. Note that the present approach allows us to directly extend the formulation to columns with varying cross-section.

Different boundary conditions for the solutions of linearized equations will be taken into account. For the points at which the elements bond we demand the equality of displacements and rotations and the equilibrium of the internal forces. At the delamination ends, e.g. at the points T_2 and T_3 (see Figure 1) we thus have:

$$\delta u_1(L_1) = \delta u_2(0) = \delta u_3(0) \tag{86}$$
$$\delta w_1(L_1) = \delta w_2(0) = \delta w_3(0) \tag{87}$$
$$\delta \varphi_1(L_1) = \delta \varphi_2(0) = \delta \varphi_3(0) \tag{88}$$
$$\delta R_{X,1}(L_1) = \delta R_{X,2}(0) + \delta R_{X,3}(0) \tag{89}$$
$$\delta R_{Z,1}(L_1) = \delta R_{Z,2}(0) + \delta R_{Z,3}(0) \tag{90}$$
$$\delta M_1(L_1) = \delta M_2(0) + \delta M_3(0) \tag{91}$$

and

$$\delta u_2(L_2) = \delta u_3(L_2) = \delta u_4(0) \tag{92}$$
$$\delta w_2(L_2) = \delta w_3(L_2) = \delta w_4(0) \tag{93}$$
$$\delta \varphi_2(L_2) = \delta \varphi_3(L_2) = \delta \varphi_4(0) \tag{94}$$
$$\delta R_{X,2}(L_2) + \delta R_{X,3}(L_2) = \delta R_{X,4}(0) \tag{95}$$
$$\delta R_{Z,2}(L_2) + \delta R_{Z,3}(L_2) = \delta R_{Z,4}(0) \tag{96}$$
$$\delta M_2(L_2) + \delta M_3(L_2) = \delta M_4(0). \tag{97}$$

For each of the analyzed columns one end (point T_1) is fixed in axial direction, and at the other end (point T_4) the axial force is zero:

$$\delta u_1(0) = 0 \tag{98}$$
$$\delta R_{X,4}(L_4) = 0. \tag{99}$$

Four different boundary conditions for columns will be analyzed:

(i) Clamped at one end free at the other (cantilever)

$$\delta w_1(0) = 0 \tag{100}$$
$$\delta \varphi_1(0) = 0 \tag{101}$$
$$\delta R_{Z,4}(L_4) = 0 \tag{102}$$
$$\delta M_4(L_4) = 0. \tag{103}$$

(ii) Pinned at both ends (simply supported)

$$\delta w_1(0) = 0 \tag{104}$$
$$\delta w_4(L_4) = 0 \tag{105}$$
$$\delta M_1(0) = 0 \tag{106}$$
$$\delta M_4(L_4) = 0. \tag{107}$$

(iii) Clamped column at one end, pinned at the other

$$\delta w_1(0) = 0 \tag{108}$$
$$\delta \varphi_1(0) = 0 \tag{109}$$
$$\delta w_4(L_4) = 0 \tag{110}$$
$$\delta M_4(L_4) = 0. \tag{111}$$

(iv) Clamped at both ends

$$\delta w_1(0) = 0 \tag{112}$$
$$\delta \varphi_1(0) = 0 \tag{113}$$
$$\delta w_4(L_4) = 0 \tag{114}$$
$$\delta \varphi_4(L_4) = 0. \tag{115}$$

The total set of equations consist of 18 continuity conditions (86)–(97) and 6 boundary conditions; totally 24 equations for 24 unknowns: α_i, β_i, A_i, B_i, C_i, D_i, $i = 1, \ldots, 4$. We are interested only in non-trivial solutions, where all the parameters are not equal to zero. The equations are linear and homogenous, thus they can be written in the form

$$\boldsymbol{K}\boldsymbol{\alpha} = \mathbf{0},$$

where $\boldsymbol{K}$ denotes the 24×24 matrix of coefficients and $\boldsymbol{\alpha}$ the vector of 24 unknowns. For solutions, where $\boldsymbol{\alpha} \neq \mathbf{0}$, the lowest value of F is sought, such that $\det \boldsymbol{K} = 0$. The lowest pair (F, ε) is sought such that the determinant of the system of equations vanishes with the determinant of the cross-sectional tangent matrix being positively definite ($c > 0$). The analytical expressions for $\det \boldsymbol{K}$ are unfortunately too complicated to be presented as closed formulae; some of the results, obtained by the above algorithm are presented in next section. For further details on calculus of critical points and their classification see the paper by Planinc and Saje [19].

5 Results and discussion

The critical force of the delaminated column is dependent on various parameters. Here, the influence of the delamination length, delamination position, shear modulus, and slenderness ratio is analyzed. Some of the results and parameters are normalized in order to present the buckling behaviour and the influence of various parameters more evidently. In all the examples the obtained critical force, e.g. the buckling load, is normalized with respect to the value of the classical Euler's result. In order to study the shear effect the elastic to shear modulus ratio has been varied. The present results are presented for:

i) $E/G = 0$; shear incompressible material, commonly taken in studying the buckling and postbuckling behaviour),
ii) $E/G = 2$; typical for isotropic materials, and
iii) $E/G = 6$; which is typical for composite materials, such as fibre-glass.

As the ratio is much larger for composite materials, in which the phenomena of delamination is one of typical failure modes due to production procedures, the shear effect could not be neglected for such materials. Results will be presented and discussed with respect to slenderness of the column, defined by

$$\lambda = L\sqrt{\frac{A}{I_y}}.$$

Some of the present results are compared to the results in available literature. Then thorough parametric studies are presented according to the present formulations for each type of supports.

5.1 Parametric studies for simply supported beam

To compare the present model with other authors we have employed the shear incompressible material, material with $E/G = 6$ and a modification (simplification) of the present formulation. Comparisons of normalized buckling loads of the simply supported beam are shown in Tables 1 and 2. The present results are presented for slenderness ratio $\lambda = 17.3$. It is interesting to observe that for shear incompressible material the present formulation gives larger values comparing to the classical laminate theories. The reason stems from the exact non-linear formulation employed in the present formulation. In order to validate the present results with respect to classical theories a modified buckling parameter

$$\tilde{k}^2 = -\frac{R_X}{d}$$

has been employed. For such simplification the influence of the axial strain in primary configuration in neglected, which is common to classical approach. Our results for modified buckling parameter completely agree with other authors. The present approach for incompressible material shows that the classical approach is conservative. This is not the case when the shear effect is considered. The present theory gives lower relative critical forces even for relatively slender beam. The shear effect is studied in detail in the next section. Note also that the solution, based on Reissner's beam theory, considers the extensional and bending stiffness coupling and transverse shear effect. The extensional and bending stiffness coupling results in larger critical forces with respect to classical Euler's solution when transverse shear is neglected ($G = \infty$).

Table 1
Normalized buckling loads of simply supported beam: comparison table 1.

	$\mu = 0$				$\mu = 0.2$			
d.l.	0.2	0.4	0.6	0.8	0.2	0.4	0.6	0.8
Simitses et.al. [22]	0.9997	0.9912	0.9343	0.7867	0.9997	0.9902	0.9198	0.7264
Parlapalli, Shu [18]	0.9997	0.9912	0.9343	0.7867				
Lim, Parsons EM [14]					0.9997	0.9902	0.9198	0.7264
Lim, Parsons FE [14]					0.9997	0.9902	0.9198	0.7264
Present simplified	0.99974	0.99122	0.93432	0.78673	0.99972	0.99023	0.91981	0.72636
Present $G = \inf$	1.03498	1.02585	0.96495	0.80822	1.03496	1.02478	0.94946	0.74460
Present $G = E/6$	0.85176	0.84543	0.80285	0.68970	0.85174	0.84469	0.79190	0.64223

d.l.=relative delamination length, μ=relative vertical position of delamination with respect to centroid

Table 2
Normalized buckling loads of simply supported beam: comparison table 2.

	$\mu = 0.4$				$\mu = 0.8$			
d.l.	0.2	0.4	0.6	0.8	0.2	0.4	0.6	0.8
Simitses et.al. [22]	0.9997	0.9827	0.8149	0.5118	0.9723	0.2494	0.1109	0.0624
Parlapalli, Shu [18]	0.9997	0.9852	0.9149	0.5118	0.9723	0.2494	0.1109	0.0624
Present simplified	0.99965	0.98515	0.81492	0.51179	0.97228	0.24938	0.11087	0.06237
Present $G = \inf$	1.03488	1.01934	0.83803	0.52071	1.00554	0.25146	0.11127	0.06250
Present $G = E/6$	0.85169	0.84092	0.71163	0.46726	0.83131	0.23784	0.10847	0.06159

d.l.=relative delamination length, μ=relative vertical position of delamination with respect to centroid

As expected the relative buckling load reduces by increasing the delamination length and/or by moving the delamination towards the cross-section's boundary. The effect of delamination length and relative vertical position on normalized buckling load is presented by a surface in Figure 2. It is evident from Figure 2, that the relationship between buckling load and both parameters is non-linear. For relatively short delamination ($d.l. \leq 0.3$), the normalized buckling load is mostly independent on their vertical position. This is not the case only for the delaminations that are very close to the boundary ($\mu > 0.8$); for which normalized buckling load rapidly decreases. For relatively longer delaminations even relatively small vertical asymmetry of delamination results in considerable reduction of normalized buckling load. Note that in Figure 2 elastic to shear ratio is taken to be 6 and that the slenderness ratio is approximately 70. The results for lower slenderness are quite different. In order to make comparisons more clear results for various shear moduli are presented as two dimensional charts in Figures 3 and 4.

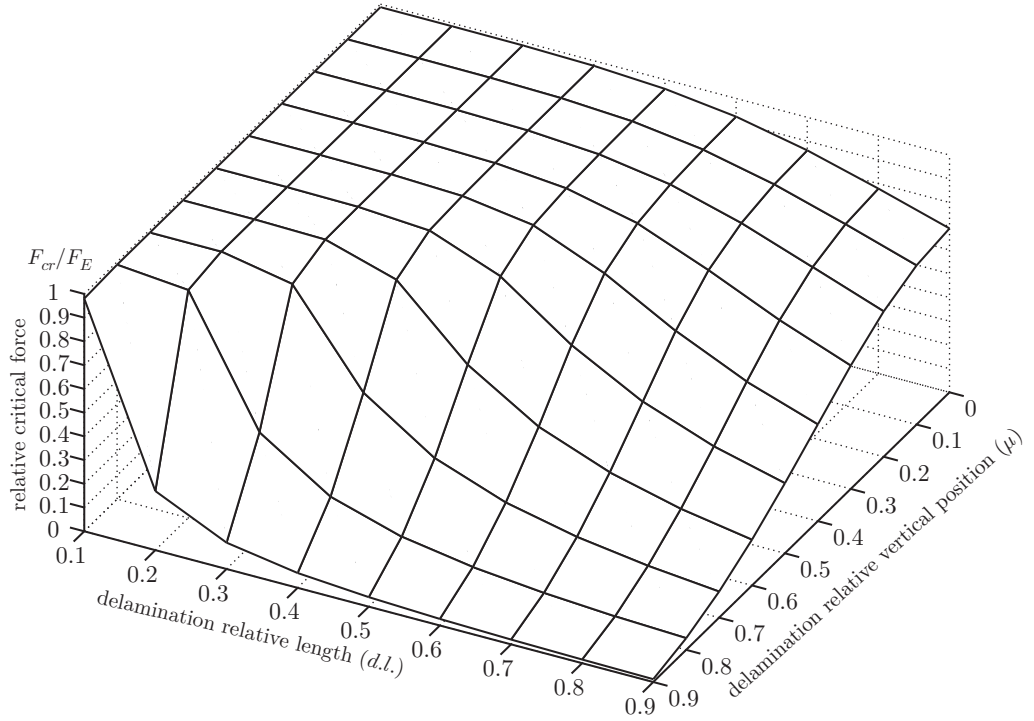

Fig. 2. Relative critical force vs. relative delamination length and vertical position.

In Figure 3 the normalized buckling load is presented for various relative delamination lengths. Nine cases are considered introducing different shear moduli and delamination vertical positions. From all the charts we observe that by increasing the delamination length the relative buckling load decreases. However the reduction of relative buckling load is non-linear and is strongly dependent on the delamination position. For symmetric delamination the slenderness-load curves are almost identical for $d.l. \leq 0.3$; for lager delam-

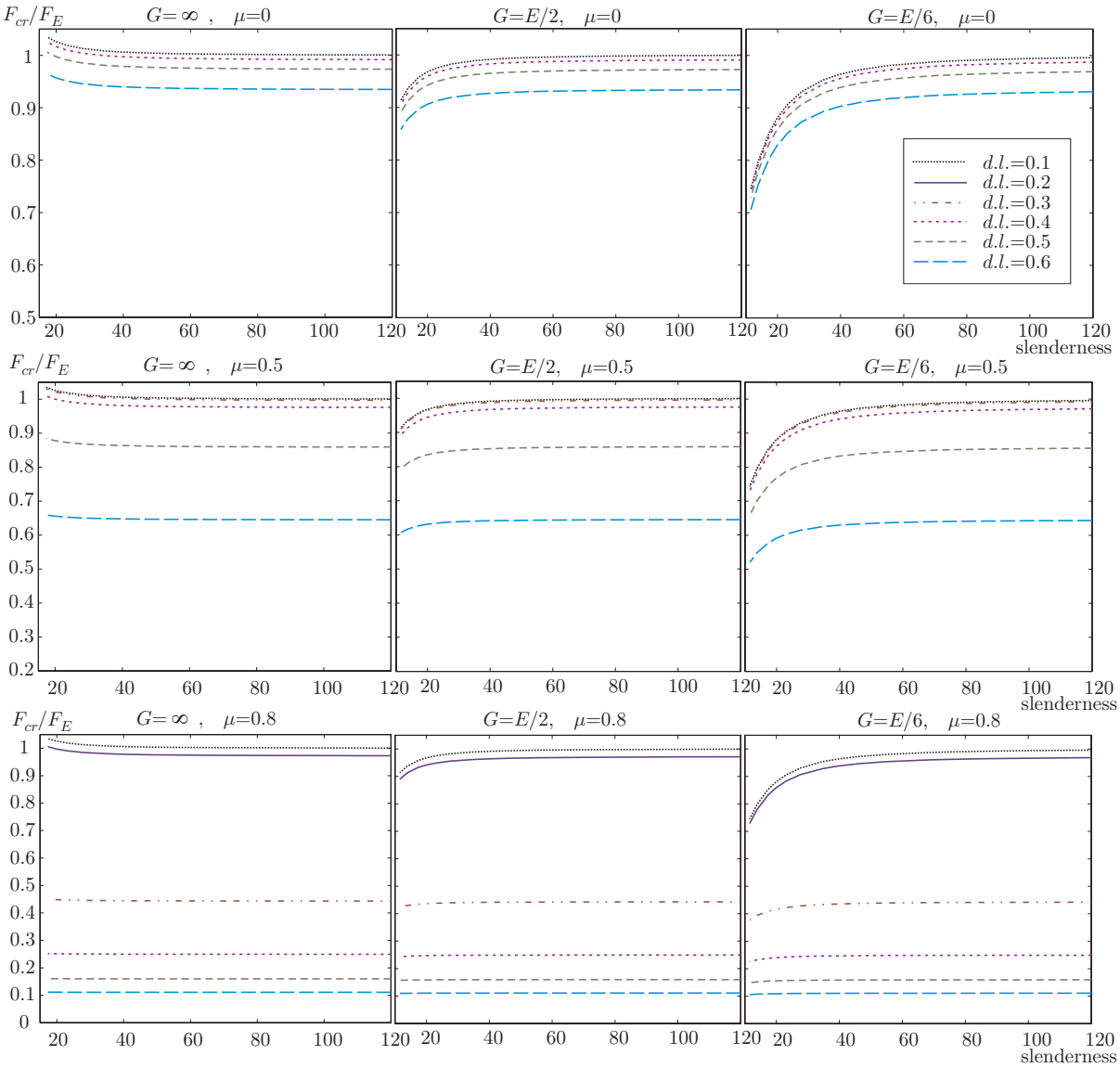

Fig. 3. Simply supported beam: relative critical force vs. slenderness ratio for various delamination lengths ($d.l.$), shear moduli (G) and delamination positions (μ).

ination lengths the distance between the curves raises. For delamination of the column at the quarter of the height ($\mu = 0.5$) first three curves are still very close together, but the distances between the other change. This is even more evident for the delamination at 10% of the height ($\mu = 0.8$), where the normalized critical forces reduce most rapidly between $d.l. = 0.2$ and $d.l. = 0.3$. Results for larger delaminations are, however, more closer to each other.

In Figure 4 the normalized buckling load is presented for various relative delamination vertical positions. Nine cases are considered introducing different shear moduli and relative lengths of delamination. Again it could be confirmed

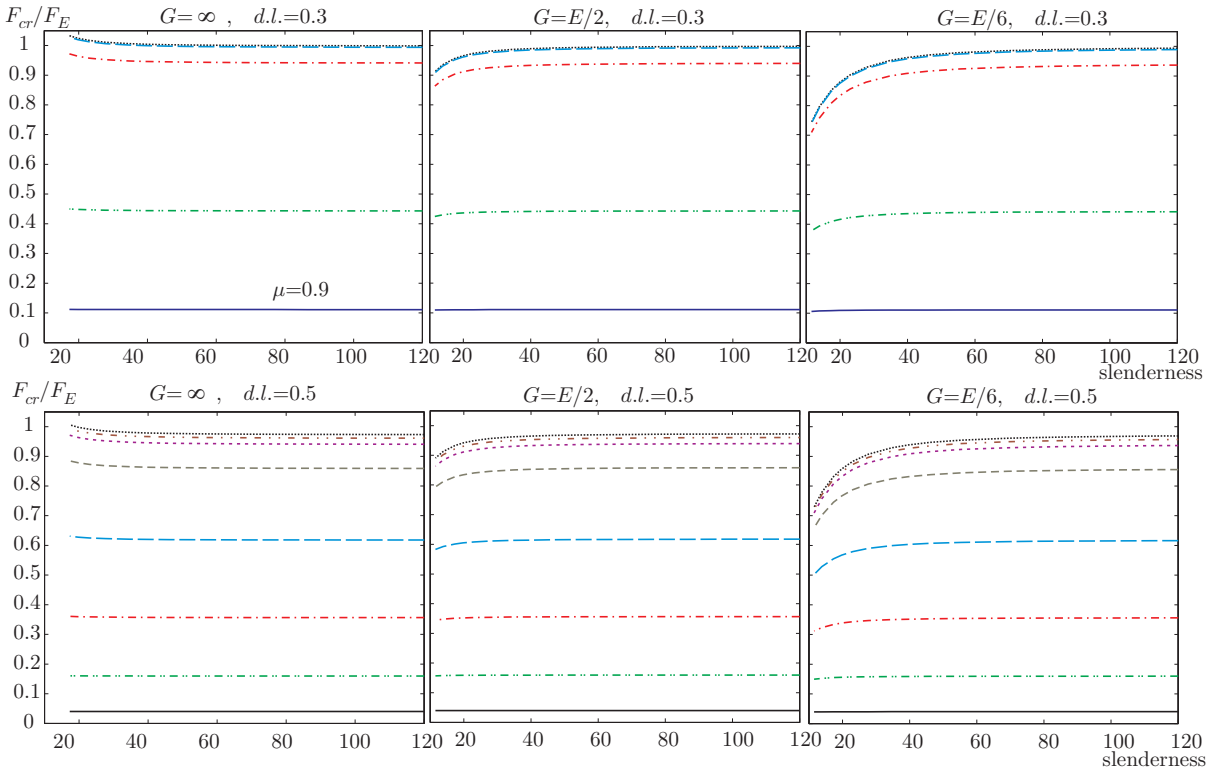

Fig. 4. Simply supported beam: relative critical force vs. slenderness ratio for various delamination positions (μ), shear moduli (G) and delamination lengths ($d.l.$).

that relatively short delamination are insensitive to moderate asymmetry of delamination position. This is not the case for longer delaminations, where the vertical asymmetry seems to be crucial.

Another important issue, evident form Figures 3 and 4, is the relationship between the slenderness ratio and the shear effect. The shear effect could not be neglected for relatively stocky columns ($\lambda < 50$). When the material is shear incompressible ($G = \infty$), the relative buckling load is almost independent on the slenderness. The slight increase in relative buckling load for stocky columns is due to the non-linear model where the axial deformation is properly taken into account. For typical isotropic materials ($G = E/2$), the shear effect is observed for thick columns ($\lambda < 20$) and relatively short delaminations. The shear effect reduces the relative buckling load. When the composite material is applied, the shear to elastic modulus is even larger, which results in considerably lover critical forces for slenderness lower than 60. The effect is stronger for shorter delamination positioned nearer the symmetry axis of the cross-section. The shear effect could reduce the normalized buckling load for more than 20% when slenderness ratio is approximately 15.

5.2 Study of various boundary conditions

The parametric studies presented above have been preformed for simply supported column. Different boundary conditions, especially non-symmetric boundary conditions can have considerable influence on the quantitative and qualitative buckling of the delaminated column. In all of the results columns with slenderness ratio 34.6 and longitudinally symmetrical delamination were studied. Different support types were analyzed with respect to transverse shear effect (introduced by shear modulus G), vertical delamination position μ, and delamination length $d.l.$ In Table 3 the comparison between different support types is shown for various combinations of parameters.

Results for different support types, although normalized with respect to Euler's critical force for the same boundary conditions, differ considerably. The variation of the analyzed parameters could have substantially dissimilar values when different boundary conditions are applied. It is common for all the support types that by increasing the delamination length the relative critical force is decreased. By increasing the shear modulus the relative critical force is increased in all the cases. For most cases the relative critical force is decreased by increasing the vertical asymmetry of delamination (parameter μ). It is important to observe that this is not always the case when asymmetrical boundary conditions are applied (clamped-pined and cantilever column). For all the parameter combinations the highest relative buckling load is almost always obtained when the column is clamped only at one end, thus cantilever column is the most conservative for variations of parameters. On the other hand the clamped-pinned column gives the lowest results for critical force when analyzing relatively short delaminations near the neutral axis. For longer delaminations and higher values of μ clamped-clamped column gives considerably lower results as the clamped-pinned one.

Buckling mode shapes for various boundary conditions are presented in Figure 5. We should point out that for all cases the matrix rank of the entire set of equations was equal to 23 at the critical load. Thus, a single eigenvector defines the corresponding buckling mode. We could agree from Figure 5 that the modes could be classified to global, where the buckling of entire column is dominant with respect to delamination, local, where only delamination occurs, and mixed, where both global and local buckling take place. Note that this classification is based entirely on the appearance of buckling shapes and has not been defined theoretically. Note also that by analyzing the matrix rank of boundary and continuity conditions separately this phenomenon could not be described, as for all the cases the separated ranks were 6 and 18, respectively. We could observe that vertically symmetrical delaminations have only minor affect on the buckling shapes; the global buckling occurs. By reducing the height of the layers, the delamination appears together with global

Table 3
Normalized buckling loads for various support types.

G	μ	$d.l.$	pinned-pinned	clamped-clamped	clamped-pinned	clamped-free
$E/6$	0	0.2	0.9534	0.8487	0.8732	0.9827
$E/6$	0	0.5	0.9289	0.6129	0.5878	0.9114
$E/6$	0	0.8	0.7575	0.3293	0.4107	0.7355
$E/2$	0	0.2	0.9885	0.9537	0.9378	0.9921
$E/2$	0	0.5	0.9623	0.6690	0.6153	0.9195
$E/2$	0	0.8	0.7797	0.3459	0.4241	0.7408
∞	0	0.2	1.0081	1.0305	0.9777	0.9970
∞	0	0.5	0.9808	0.7060	0.6312	0.9237
∞	0	0.8	0.7919	0.3556	0.4316	0.7435
$E/6$	0.2	0.2	0.9534	0.8483	0.8763	0.9831
$E/6$	0.2	0.5	0.9250	0.5137	0.6126	0.9215
$E/6$	0.2	0.8	0.7013	0.2318	0.3849	0.7644
$E/2$	0.2	0.2	0.9885	0.9532	0.9426	0.9928
$E/2$	0.2	0.5	0.9580	0.5534	0.6445	0.9304
$E/2$	0.2	0.8	0.7204	0.2402	0.3971	0.7708
∞	0.2	0.2	1.0081	1.0299	0.9841	0.9978
∞	0.2	0.5	0.9764	0.5786	0.6631	0.9350
∞	0.2	0.8	0.7308	0.2448	0.4037	0.7741
$E/6$	0.8	0.2	0.9283	0.2380	0.4651	0.9866
$E/6$	0.8	0.5	0.1584	0.0396	0.0775	0.6325
$E/6$	0.8	0.8	0.0622	0.0156	0.0304	0.2486
$E/2$	0.8	0.2	0.9616	0.2467	0.4822	0.9964
$E/2$	0.8	0.5	0.1593	0.0399	0.0780	0.6365
$E/2$	0.8	0.8	0.0623	0.0156	0.0305	0.2492
∞	0.8	0.2	0.9802	0.2516	0.4918	1.0014
∞	0.8	0.5	0.1598	0.0400	0.0782	0.6385
∞	0.8	0.8	0.0624	0.0156	0.0305	0.2495

$d.l.$=relative delamination length, μ=relative vertical position of delamination with respect to centroid

buckling, but for very thin and long delaminations only the thin layer buckles, which results in local buckling shape. The comparison between various boundary conditions shows considerable dissimilarities in mode shapes for otherwise identical columns. We should point out that for relatively short delaminations the longitudinal asymmetry could considerably affect the global mode shape, as observed for clamped-clamped beam in Figure 5. Note also that the transverse shear does not affect the buckling mode shapes (it affects only the

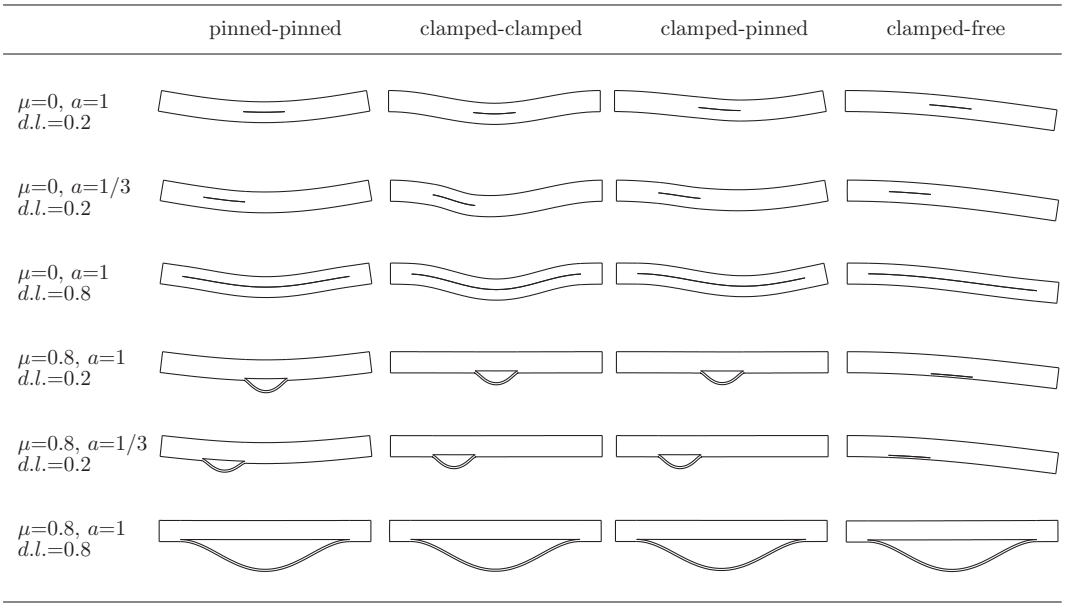

d.l.=relative delamination length, μ=relative vertical position of delamination with respect to centroid
a=longitudinal asymmetry

Fig. 5. Buckling modes of various delaminated columns.

magnitudes of buckling forces), thus the comparisons are not presented here.

5.3 Study of longitudinal asymmetry

The shear effect is only rarely considered in delamination models. Here we compare the results of the present theory to the ones obtained by Chen [3] for the beam clamped at both ends. In [3] the shear deformation parameter introduced is dependent on length to thickness ratio. In present approach the shear effect is applied directly with shear modulus G. The shear deformation parameter 0.2 from [3] is thus adequately replaced by elastic to shear modulus ratio. For the present length to thickness ratio $h/L = 0.1$ the size of E/G, accordant to [3], is 6.8. Tables 4 and 5 show good agreement between both results (up to 3 significant digits). The differences stem from different approach applied here with respect to the one in [3]. Note that the delamination is normally positioned to the middle of the beam's length and different thicknesses are studied. Our results show that the longitudinal position of delamination can be of considerable influence. The present results in Tables 4 and 5 are shown for $L_1 : L_4 = 1 : 1$, $L_1 : L_4 = 1 : 2$, and $L_1 : L_4 = 1 : 3$. We can observe that the results for longitudinally symmetric delamination ($L_1 = L_4$) can be non-conservative and the proper consideration of delamination position can be of great importance.

Table 4
Normalized buckling loads of clamped-clamped beam: comparison table 1.

	$\mu = 0$				$\mu = 0.2$			
d.l.	0.2	0.4	0.6	0.8	0.2	0.4	0.6	0.8
Chen [3]	0.99556	0.85606	0.54114	0.35142	0.99504	0.7883	0.41239	0.24281
Chen + shear [3]	0.83025	0.73092	0.48829	0.32834	0.82989	0.68094	0.38097	0.23156
Present	1.03049	0.87316	0.55113	0.35558	1.02994	0.80988	0.41814	0.24478
Present + shear, 1 : 1	0.83232	0.70267	0.48558	0.32633	0.83195	0.67951	0.37861	0.23031
Present + shear, 1 : 2	0.76136	0.57163	0.46955	0.32590	0.76880	0.58756	0.37765	0.23034
Present + shear, 1 : 3	0.72973	0.52076	0.45151	0.32536	0.73942	0.54067	0.37630	0.23038

d.l.=relative delamination length, μ=relative vertical position of delamination with respect to centroid

Table 5
Normalized buckling loads of clamped-clamped beam: comparison table 2.

	$\mu = 0.4$				$\mu = 0.8$			
d.l.	0.2	0.4	0.6	0.8	0.2	0.4	0.6	0.8
Chen [3]	0.99239	0.53138	0.24353	0.13901	0.24953	0.06242	0.02776	0.01562
Chen+shear [3]	0.82804	0.48033	0.23222	0.13525	0.23767	0.06165	0.02761	0.01557
Present	1.02710	0.54101	0.24551	0.13965	0.25162	0.06255	0.02778	0.01563
Present + shear, 1 : 1	0.83005	0.47763	0.23096	0.13473	0.23637	0.06153	0.02758	0.01556
Present + shear, 1 : 2	0.78610	0.47873	0.23120	0.13476	0.23640	0.06154	0.02758	0.01556
Present + shear, 1 : 3	0.76335	0.48034	0.23151	0.13480	0.23644	0.06154	0.02758	0.01556

d.l.=relative delamination length, μ=relative vertical position of delamination with respect to centroid

The phenomenon of relative critical force reduce by asymmetrical longitudinal delamination position has been studied for columns with slenderness ratio 35 and several vertical delamination positions. The transverse shear effect was studied by taking different values of shear moduli ($G = \infty$ and $G = E/6$). In the study symmetric delamination was compared to the cases with delamination positioned at 1/4 and 1/8 of the non-delaminated length ($L_1 : L_4 = 1 : 3$, $L_1 : L_4 = 1 : 7$), respectively. Various boundary conditions were taken into account.

The results for clamped-clamped columns are shown in Figure 6. We can observe that the increase of longitudinal asymmetry affects the most the columns with medium-sized delaminations when the delamination is at the centroid of

the column ($\mu = 0$). For delaminations asymmetric to the height of the column, the effect is reduced and can be neglected for larger values of μ. It is however interesting that by vertically positioning the delamination towards the boundary of the cross-section shorter delaminations indicate to be more sensitive on longitudinal position. The qualitative influence of longitudinal delamination position is analogous when the shear incompressible material is applied, but the quantitative values of relative critical forces (dotted lines) can be non-conservative, especially for shorter delaminations. Note that due to symmetry of boundary conditions the identical results are obtained for delaminations with $L_1 : L_4 = 3 : 1$ and $L_1 : L_4 = 7 : 1$, respectively. For non-symmetric boundary conditions no such symmetry of results according to the mid-span of the beam is expected, as we will confirm in further examples.

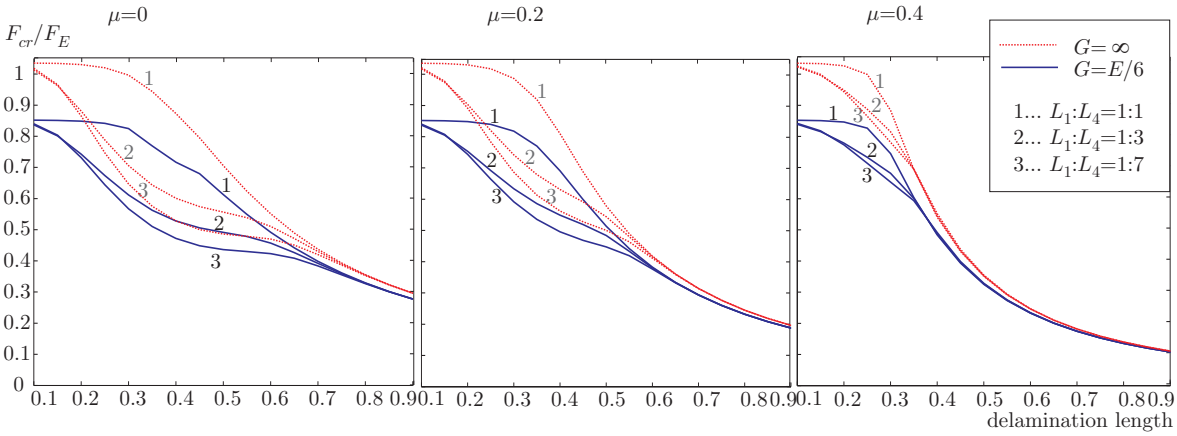

Fig. 6. Clamped-clamped column: relative critical force vs. delamination length for various delamination longitudinal positions.

Results for columns, clamped at one end, pinned at the other, are shown in Figure 7. From Figure 7 it is obvious that the longitudinal delamination position could have considerable influence on buckling loads particularly for vertically symmetrical delaminations and moderate vertical asymmetry ($\mu < 0.5$). In contrast to previous example the delamination centered at mid-span of the column's length does not give the largest buckling loads. Generally by moving the delamination from the clamped end ($x = 0$) to the pinned one ($x = L$), the relative critical force raises. It is, however, interesting to observe that relatively short delaminations when positioned closer to mid-span ($L_1 : L_4 = 3 : 1$) can give larger buckling loads as when positioned nearer the pinned end ($L_1 : L_4 = 7 : 1$). The same phenomenon, but not so distinctive in values of relative buckling loads, is observed by moving the delamination to the clamped end. The comparisons between more realistic (solid line) and shear incompressible (dotted line) material show completely analogous behaviour of shear incompressible column with respect to the longitudinal delamination position. On the other hand, the values of relative critical forces can be non-

conservative when transverse shear is neglected.

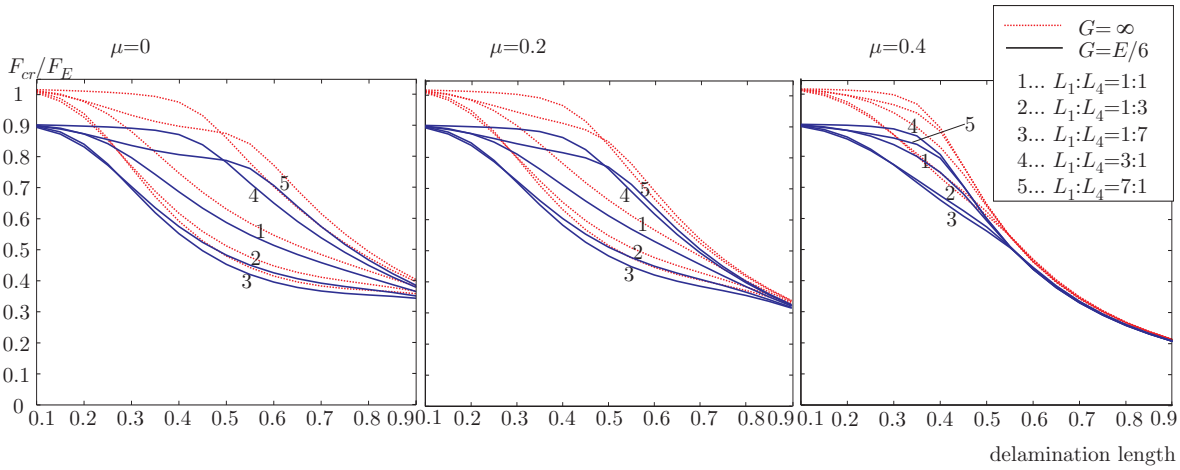

Fig. 7. Clamped-pinned column: relative critical force vs. delamination length for various delamination longitudinal positions.

Our last example is the most conservative one as the various parameters, studied in previous examples, have the lowest influence on the buckling loads. The column is now clamped at one end, free at the other (cantilever column). The delamination longitudinal position and transverse shear have only slight influence for this type of boundary conditions (see Figure 8). Delamination length and vertical position have substantial influence, but comparing to other examples their effect is lower. The most interesting issue, observed from Figure 8, is that in contrast to previous example by moving the delamination from the clamped end ($x = 0$) to the free one the relative critical forces are reduced. This is in accord with the expectation that the delamination in the neighborhood of the clamped end would have the lowest effect.

6 Conclusions

We presented the analytical approach to the buckling analysis of the asymmetric delaminated beam considering the shear effect. The essential points of the present studies are:

(i) The present formulation agrees well with the classical results for shear incompressible material.
(ii) The dependence of the buckling load on delamination length and position is strongly non-linear.
(iii) The shear effect can be substantial and can not be neglected even for isotropic material when the beams are stocky.

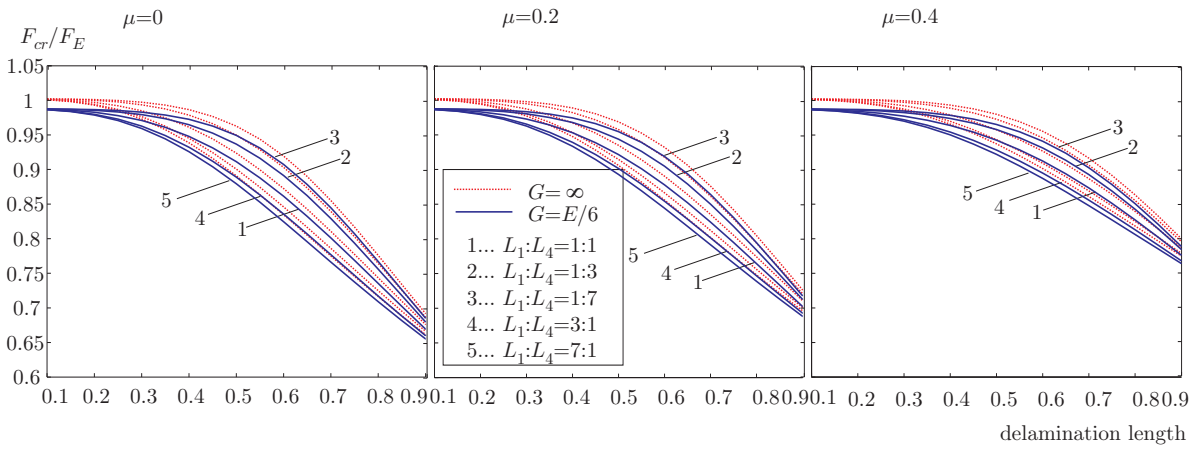

Fig. 8. Cantilever column: relative critical force vs. delamination length for various delamination longitudinal positions.

(iv) For composite materials the shear effect is substantial for low to moderate slenderness ratio. Classical approach can be most non-conservative for such cases.

(v) It is recommended that for materials with high elastic to shear modulus ratio the shear effect is properly considered.

(vi) The obtained and presented results can on behalf of their exactness serve as a benchmark for numerical methods.

Post-critical behaviour, geometric imperfections, and non-linearity of material non-analyzed in the present paper are the subject of further studies.

7 Appendix A: shear incompressible material

We will prove that for $G = \infty$, the shear dependent formulation reduces to exact formulation of shear incompressible material. When the shear deformations can be neglected, the governing equations read:

$$\delta u' - \delta\varepsilon = 0 \tag{116}$$
$$\delta w' + (1+\varepsilon)\,\delta\varphi = 0 \tag{117}$$
$$\delta\varphi' - \delta\kappa = 0 \tag{118}$$
$$\delta R_X' = 0 \tag{119}$$
$$\delta R_Z' = 0 \tag{120}$$
$$\delta M' + R_X\delta w' - (1+\varepsilon)\delta R_Z = 0 \tag{121}$$
$$C_{11}\delta\varepsilon + C_{12}\delta\kappa - \delta R_X = 0 \tag{122}$$
$$C_{21}\delta\varepsilon + C_{22}\delta\kappa - \delta M = 0. \tag{123}$$

After procedure analogous to the one in section 3.3, equation (60) is obtained once again, however the parameter k^2 is now described by

$$k^2 = -\frac{R_X}{d}(1+\varepsilon), \tag{124}$$

but the general form of the solution (61) remains the same.

From (117) and (118) we have

$$\delta\varphi = -\frac{1}{1+\varepsilon}\delta w' = -\frac{1}{1+\varepsilon}\left[k\left(A\cos kx - B\sin kx\right) + C\right] \tag{125}$$

$$\delta\kappa = -\frac{1}{1+\varepsilon}\delta w'' = \frac{1}{1+\varepsilon}k^2\left(A\sin kx + B\cos kx\right). \tag{126}$$

First derivative of (122) yields differential equation for axial displacements:

$$C_{11}\delta u'' - C_{12}\frac{1}{1+\varepsilon}\delta w''' = 0.$$

It's solution reads

$$\delta u(x) = \alpha + \beta x - \frac{C_{12}}{C_{11}}\frac{1}{1+\varepsilon}k\left(B\sin kx - A\cos kx\right).$$

From (116) we now have

$$\delta\varepsilon = \beta - \frac{C_{12}}{C_{11}}\frac{1}{1+\varepsilon}k^2\left(A\sin kx + B\cos kx\right).$$

After inserting $\delta\varepsilon$ and $\delta\kappa$ into (122) and (123) and some simplification we get

$$\delta R_X = C_{11}\beta \tag{127}$$

$$\delta M = C_{21}\beta + \frac{1}{1+\varepsilon}dk^2\left(A\sin kx + B\cos kx\right). \tag{128}$$

Inserting the expressions for δM, δw, and δR_Z into (121) results in

$$\delta R_Z = \frac{1}{1+\varepsilon}R_X C. \tag{129}$$

The comparison shows the complete analogy between no-shear and shear theory, where the shear effect can be fully considered only by proper modification of the buckling parameter k.

References

[1] Z. P. Bažant, L. Cedolin, *Stability of Structures: Elastic, Inelastic, Fracture and Damage Theories*, Oxford University Press, New York, 1991.

[2] H. Chai, C. D. Babcock, W. B. Knauss, *One dimensional modeling of failure in laminated plates by delamination buckling*, Int. J. of Solids Structures 17, 1069–1083, 1981.

[3] H.-P. Chen, *Shear deformation theory for compressive delamination buckling and growth*, AIAA Journal 29, 813–819, 1991.

[4] H.-P. Chen, *Transverse shear effects on buckling and postbuckling of laminated and delaminated plates*, AIAA Journal 31, 163–169, 1993.

[5] B. Čas, M. Saje, I. Planinc, *Non-linear finite element analysis of composite planar frames with an interlayer slip*, Computers & Structures 82, 1901–1912, 2004.

[6] B. Čas, M. Saje, I. Planinc, *Buckling of layered wood columns*, Advances in Engineering Software 38, 586–597, 2007.

[7] G.R. Cowper, *The shear coefficient in Timoshenko's beam theory.* ASME Journal of Applied Mechanics 33, 335–340, 1966.

[8] L. Euler, *Methodus inveniendi lineas curvas maximi minimive proprietate gaudentes*, Lausanne, 1744.

[9] R. Flajs, M. Saje, E. Zakrajšek, *On the existence and uniqueness of the generalized solution of Reissner's elastica*, Mathematics and Mechanics of Solids 8, 3–19, 2003.

[10] G.A. Kardomateas, D.W. Schumueser, *Buckling and post-buckling of delaminated composites under compressive loads including transverse shear effects*, AIAA Journal 26, 337–343, 1988.

[11] H.B. Keller, *Nonlinear bifurcation*, Journal of Differential Equations 7, 417–434, 1970.

[12] N. Krauberger, M. Saje, I. Planinc, S. Bratina, *Exact buckling load of a restrained RC column,* Structural Engineering and Mechanics, (to be published).

[13] Q.S. Li, *Effect of shear deformation on the critical buckling of multi-step bars*, Structural Engineering and Mechanics 15, 71–81,2003.

[14] Y.B. Lim, I.D. Parsons, *The linearized buckling analysis of a composite beam with multiple delaminations*, Int. J. of Solids Structures 30, 3085–3099, 1993.

[15] S. Moradi, F. Taheri, *Delamination buckling analysis of general laminated composite beams by differential quadrature method*, Composites: Part B 30, 503–511, 1999.

[16] K.S. Numayr, R.H. Haddad, *Analytical Solution of Buckling of Beams with Two Delaminations*, Mechanics of Composite Materials and Structures 8, 283–297, 2001.

[17] P. MSRao, D. Sylvain, D. Shu and C.N. Della, *Buckling analysis of tri-layer beams with multiple separated delaminations*, Composite Structures 66, 53–60, 2004.

[18] P. MSRao, D. Shu, *Buckling analysis of two-layer beams with an asymmetric delamination*, Engineering Structures 26, 651–658, 2004.

[19] I. Planinc, M. Saje, *A quadratically convergent algorithm for the computation of stability points: The application of the determinant of the tangent stiffness matrix*, Computer Methods in Applied Mechanics and Engineering 169, 89–105, 1999.

[20] E. Reissner, *On one-dimensional finite-strain beam theory: The plane problem*, J. Appl. Math. Phys. 23, 795–804, 1972.

[21] I. Sheinman, M. Soffer, *Post-buckling analysis of composite delaminated beams*, Int. J. of Solids Structures 27, 639–646, 1991.

[22] G.J. Simitses , S. Sallam , W.L. Yin, *Effect of delamination of axially loaded homogeneous laminated plates*, AIAA Journal 23, 1437–44, 1985.

[23] S.P. Timoshenko, J.M. Gere, *Theory of Elastic Stability*, McGraw-Hill, New York, 1961.

[24] J.L. Troutman, *Variational Calculus with Elementary Convexity*, Springer-Verlag, New York, 1983.

[25] J.T.S. Wang, H.N. Pu, C.C. Lin, *Buckling of Beam-Plates Having Multiple Delaminations*, Journal of Composite Materials 31, 1002-1025, 1997.

[26] C.M. Wang, C.Y. Wang, J.N. Reddy, *Exact solutions for buckling of structural members*, CRC Press LLC, 2005.

[27] S. Wolfram, *MATHEMATICA*, Addison – Wesley Publishing Company, 2003.

[28] D. Zupan, M. Saje, *The linearized three-dimensional beam theory of naturally curved and twisted beams: The strain vectors formulation*, Computer Methods in Applied Mechanics and Engineering 195, 4557–4578, 2006.